Electronic Supplementary Information

Investigating Interfacial Engineering of Bifunctional Electrocatalyst: Outstanding Catalytic Performance, High Intrinsic Activity and Solar to Hydrogen Conversion Efficiency

Muthukumaran Sangamithirai[a], Murugan Vijayarangan[a], Murugan Muthamildevi[a], Venkatachalam Ashok[a] and Jayaraman Jayabharathi[a]*

[a]*Department of Chemistry, Material Science Lab, Annamalai University, Annamalai Nagar, Tamil Nadu-608 002, India*

**Email id: jtchalam2005@yahoo.co.in*

Contents

SI-I: Experimental Section

SI-II: Figures

SI-III: Calculations

SI-IV: Tables and reference

SI-I: Experimental Section

Materials and Methods

Glucose ($C_6H_{12}O_6$), KOH, and 2-propanol, each with 97-99% purity, were obtained from SDFCL chemicals, while sodium bicarbonate ($NaHCO_3$) and cobalt nitrate ($Co(NO_3)_2 \cdot 6H_2O$), each with 99% purity, were sourced from Sigma-Aldrich. All reagents were used directly without additional purification, and deionized water was used throughout the experiment.

Characterization of an electrocatalyst

The morphologies and chemical compositions of catalyst samples were determined by scanning electron microscope (JEOL-JSM-IT 200) connected with an energy-dispersive X-ray spectrometer applying the 20 kV acceleration voltage. HR-TEM JOEL, JAPAN was used to record transmission electron microscope (TEM) images of the nanomaterials and selected area electron diffraction (SAED) pattern. The powder X-ray diffraction (XRD) investigated the crystal structures on a POWER-XRD EQUINOX-1000 diffractometer with Cu Kα radiation (λ=1.54056 Å). Furthermore, to determine the chemical states and compositions of catalyst samples, XPS (X-ray photoelectron spectroscopy) with a K-Alpha-KAN9954133 spectrometer (micro-focused monochromator with variable spot size), Raman spectra were registered on Invia Reflex Raman Microscope with Spectrometer and surface area and pore size measurements were analysed by the Micromertrics ASAP 2020 instrument at a temperature of 77 K.

Electrode preparation and characterization

All electrochemical measurements were carried out on a Biologic SP-300 Potentiostat electrochemical workstation, the linear sweep voltammograms (LSV) test was carried out in 1 M KOH electrolyte with a scan rate of 5 mV/s three-electrode setup. To prepare catalyst

ink, 5.0 mg of the as-prepared ID-CoMo, CoO, MoO electrocatalyst, and 30 μL Nafion (5 wt%) was evenly dispersed in 0.5 mL of propanol, and then the as-obtained solution was treated with ultrasound for 20 min. For comparison, a 0.005 mg/ml commercial IrO_2 and Pt/C suspension was made using a comparable methodology. The as-prepared catalyst ink was smeared onto Ni foam and dried at 60 ^oC for 12 h in a vacuum oven. Before coating, the NF was washed with acetone, HCl aqueous solution, deionized water and ethanol in sequence. In a three-electrode setup nickel foam (NF) as the working electrode, Ag/AgCl (3 M KCl) as reference electrode, and a platinum wire as counter electrode. Measured potentials were referred to the reversible hydrogen electrode (RHE) $\mathbf{E_{(RHE)} = E_{(Hg/HgO)} + 0.923\ V.}$ The resistances of ID-CoMo electrocatalysts were acquired from EIS tests at the overpotential of different mV (vs. RHE) in the frequency scope of 100 kHz to 10 mHz. The durability of RCoFe was tested by cyclic voltammetry (CV) and current-time (i-t) curve tests.

SI-II: Figures

Figure S1: (a) Photographs of Mechanochemical method and (b) Photographs of combustion method

(a) Mechanochemical Reaction

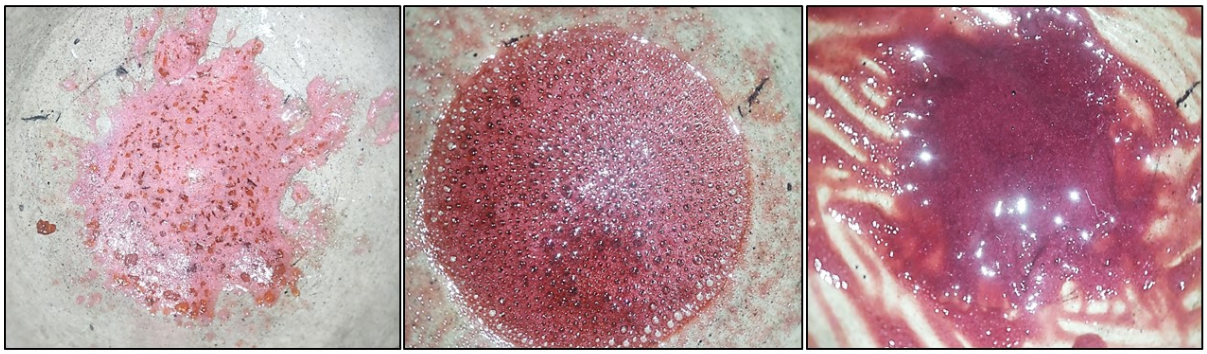

Begin to grind
Frizzy and Foamy

After 5 mins
Releasing CO_2 and H_2O

After 15 mins
Homogenous mixture

(b) Combustion Reaction

Begin to Combust

After 5mins
release of Co_2 created airpockets

Fully combust

Figure S2: Raman spectra (a) CoO and (b) carbon

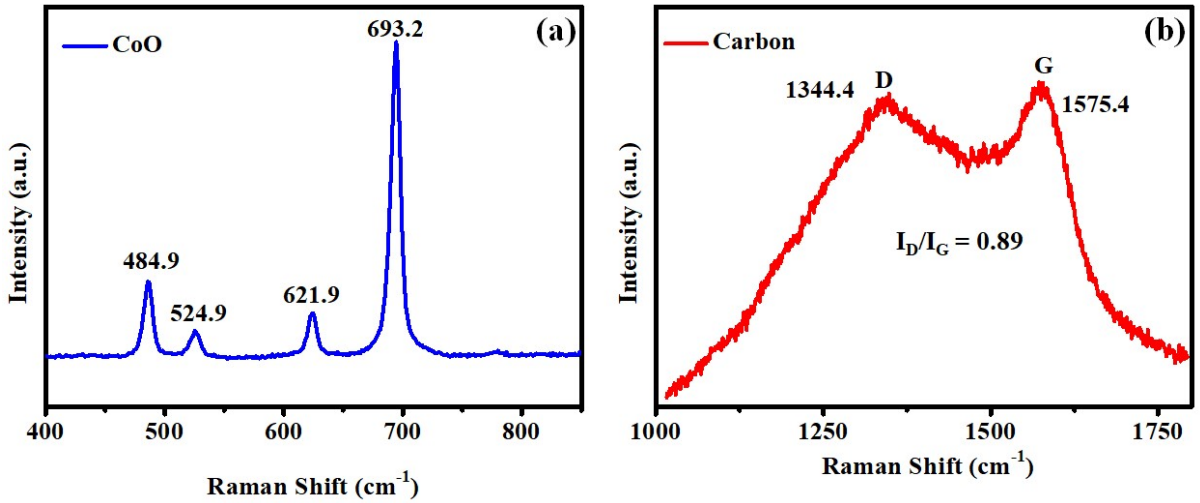

Figure S3: (a) Overall all view of elemental mapping (inset: field of view image); (b, c, d) Elemental mapping O, Co, C and (d) Energy dispersive x-ray spectra (inset: % table)

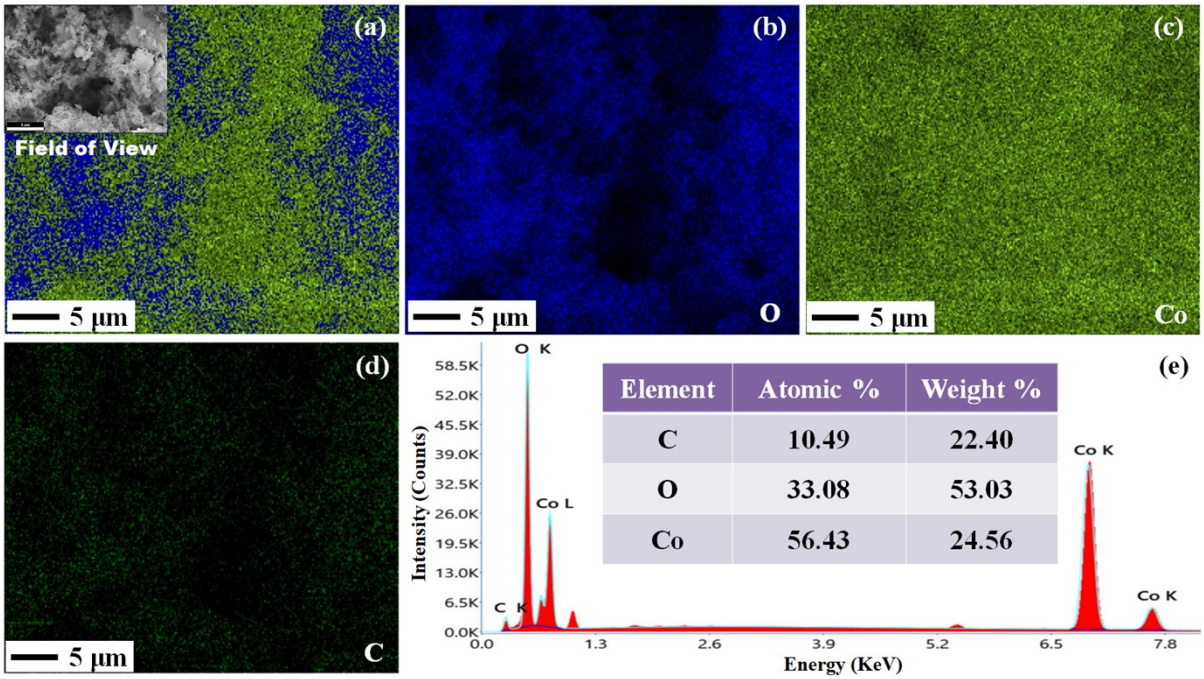

Element	Atomic %	Weight %
C	10.49	22.40
O	33.08	53.03
Co	56.43	24.56

Figure S4: (a) Porous view in HR-TEM image; (b) Carbon wrapper with core shell interface and (c) Selected area diffraction pattern

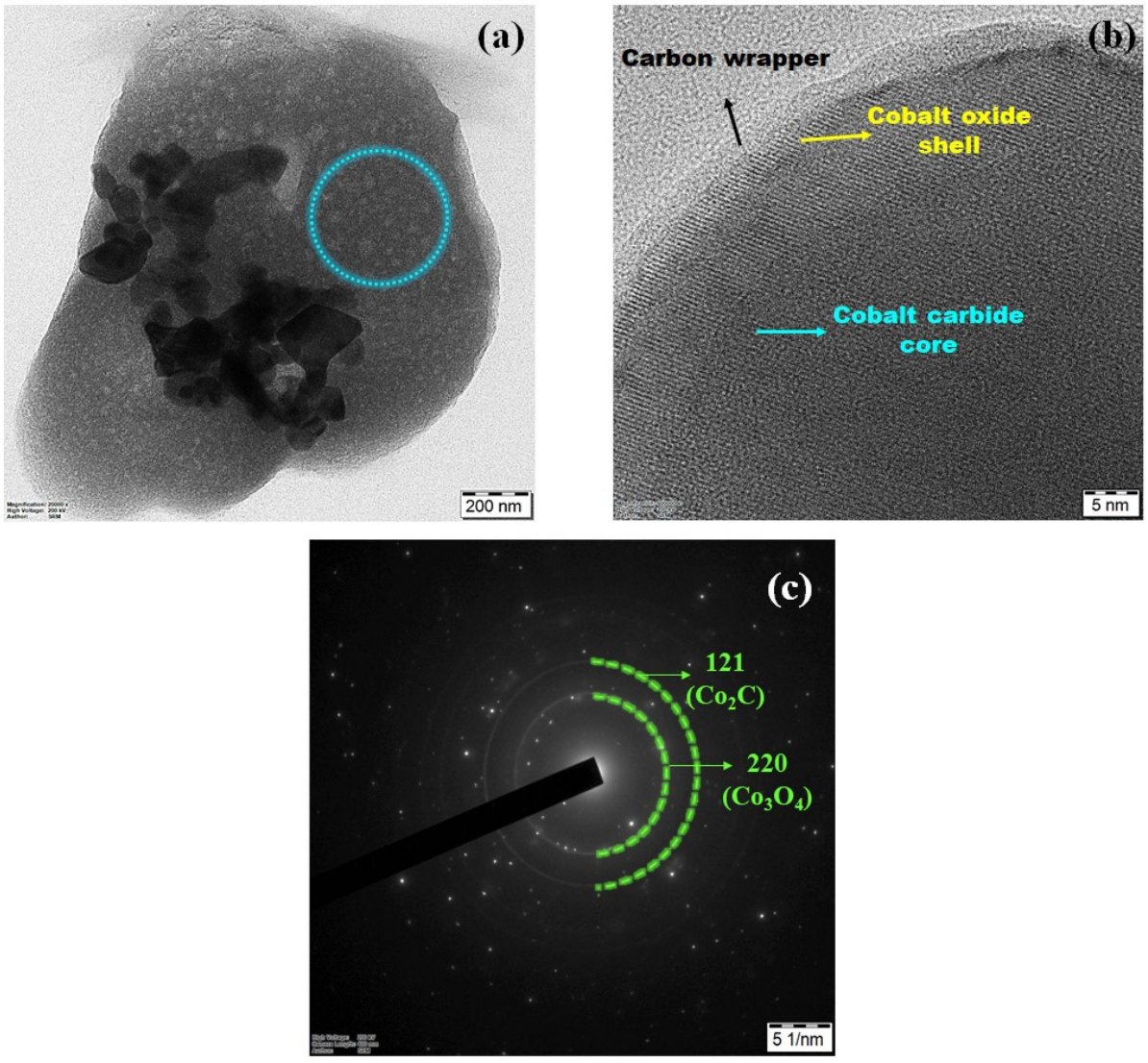

Figure S5: Different molar concentration of KOH for Co-O-C/CPs

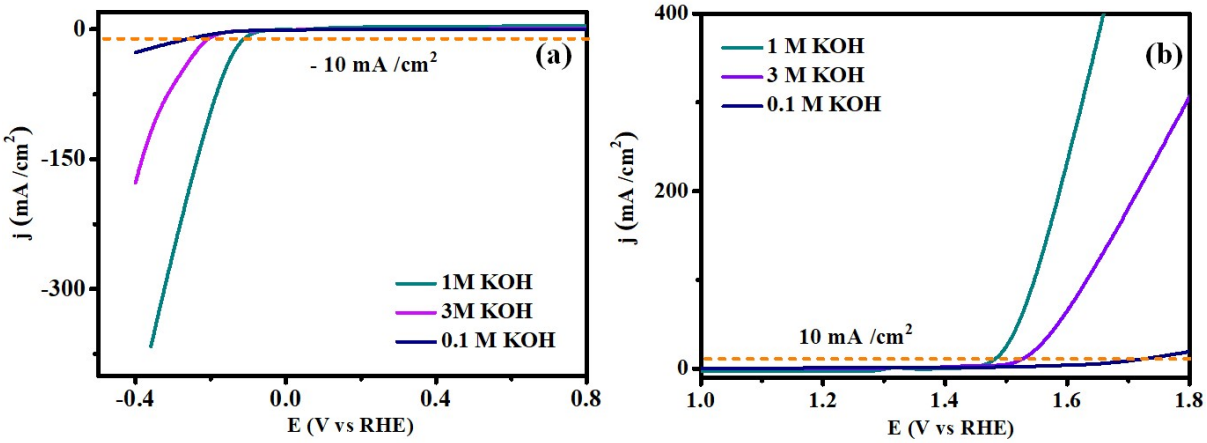

Figure S6: Electrochemical Performance of Carbon-Based Counter Electrodes

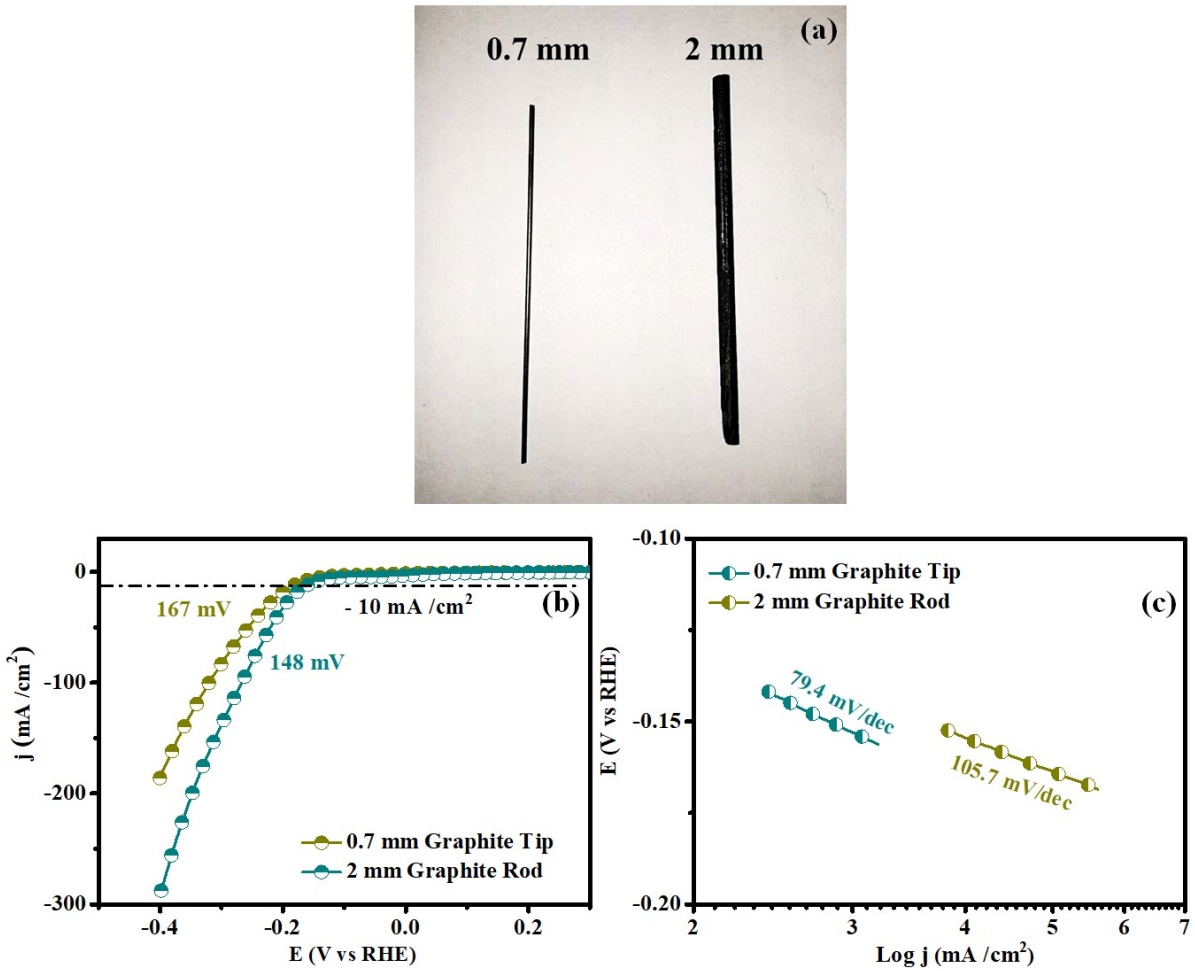

Figure S7: Electrochemical active surface area: (a) Co-O-C/CPs; (b) CoO; (c) carbon and (d) bare NF

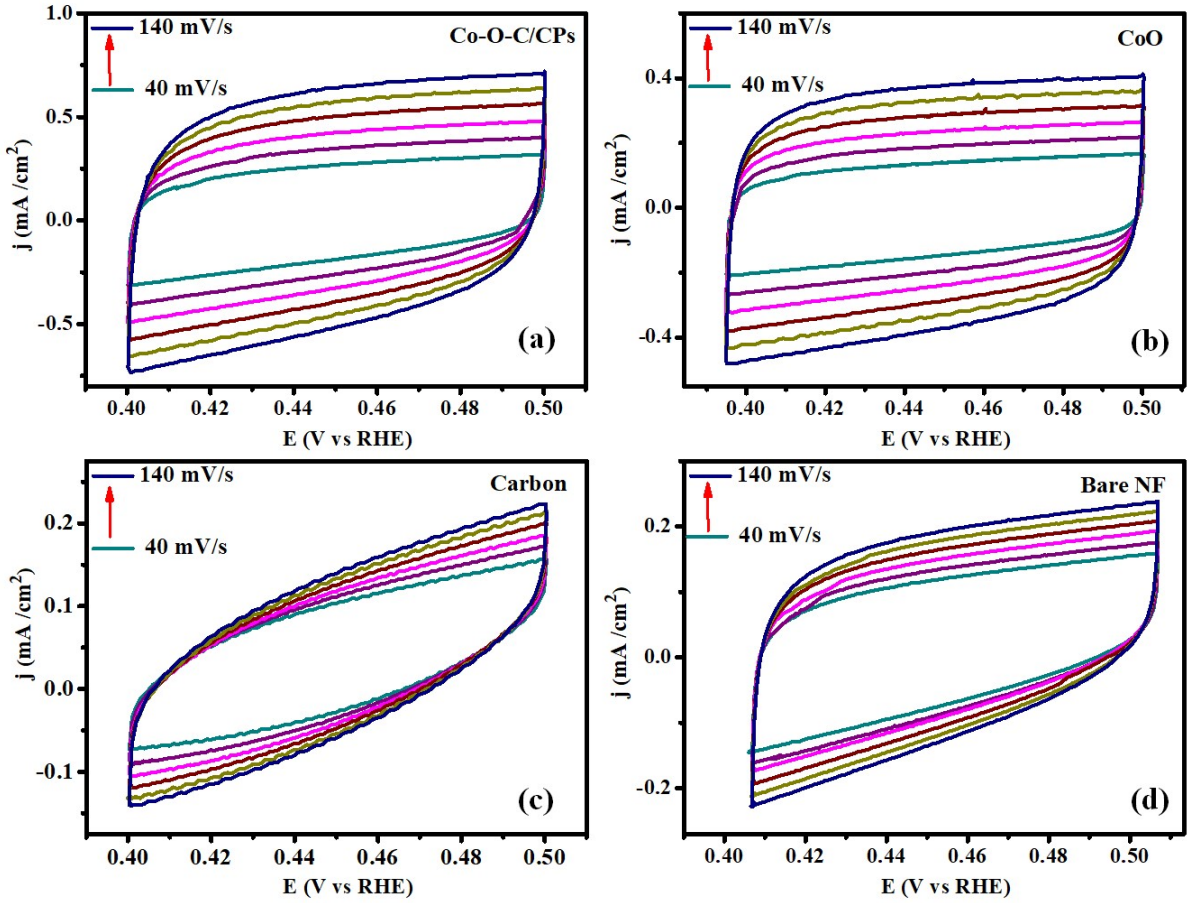

Figure S8: Turnover frequency values in radar view

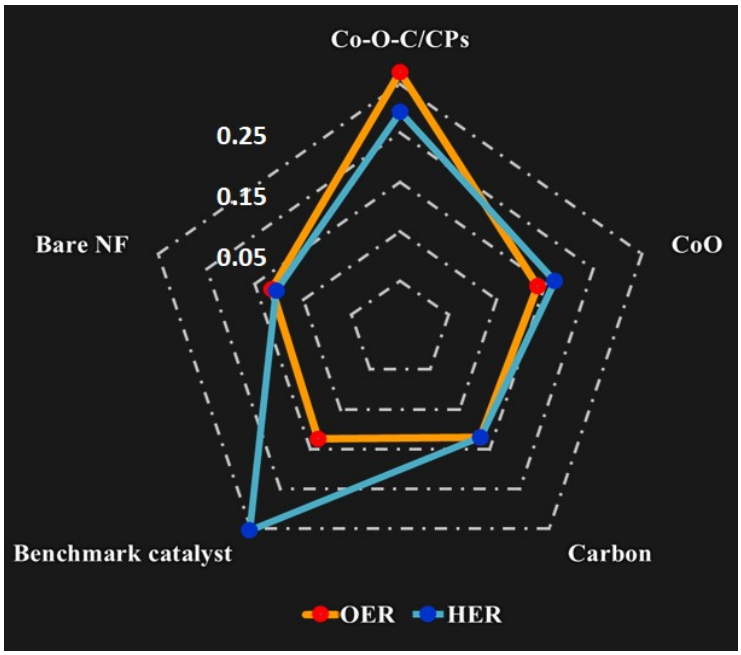

Figure S9: General solar cell water splitting setup

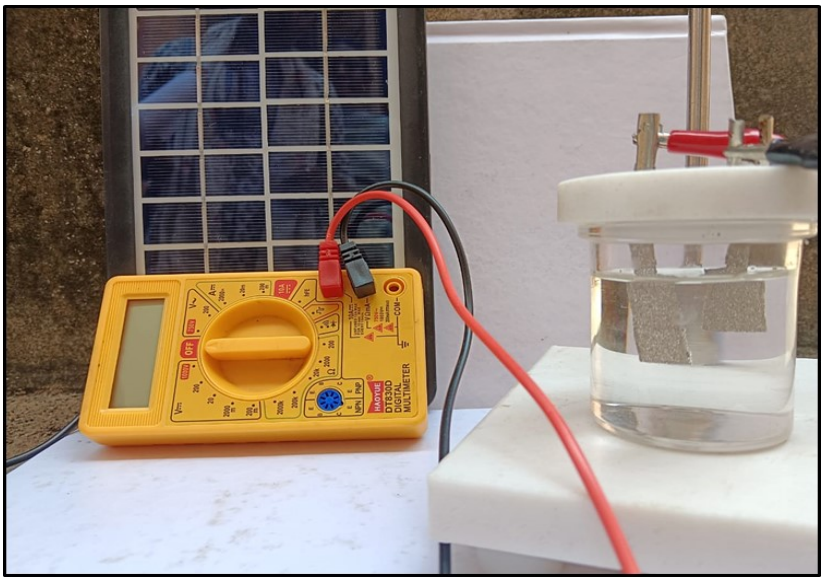

Figure S10: Field emission scanning electron microscope after OER of Co-O-C/CPs: (a) Catalyst strongly binds in NF; (b) embedded morphology; (c) Elemental mapping and (d) EDS spectra

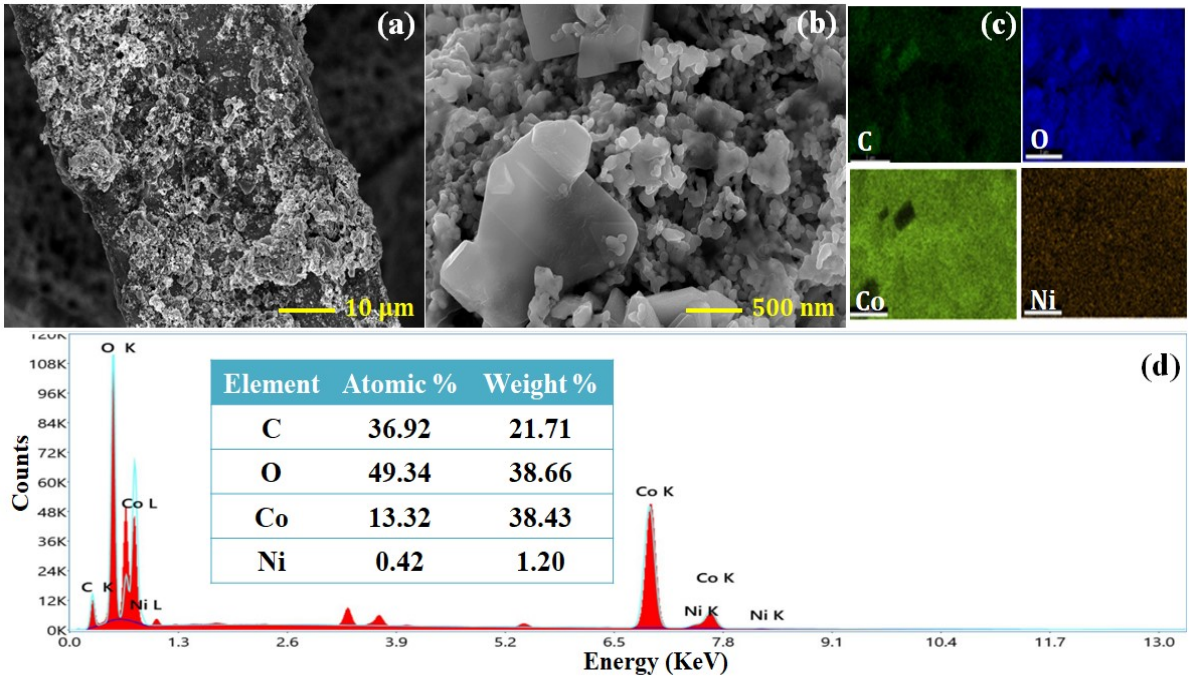

Figure S11: Field emission scanning electron microscope after HER of Co-O-C/CP: (a) Catalyst strongly binds in NF; (b) embedded morphology; (c) Elemental mapping and (d) EDS spectra

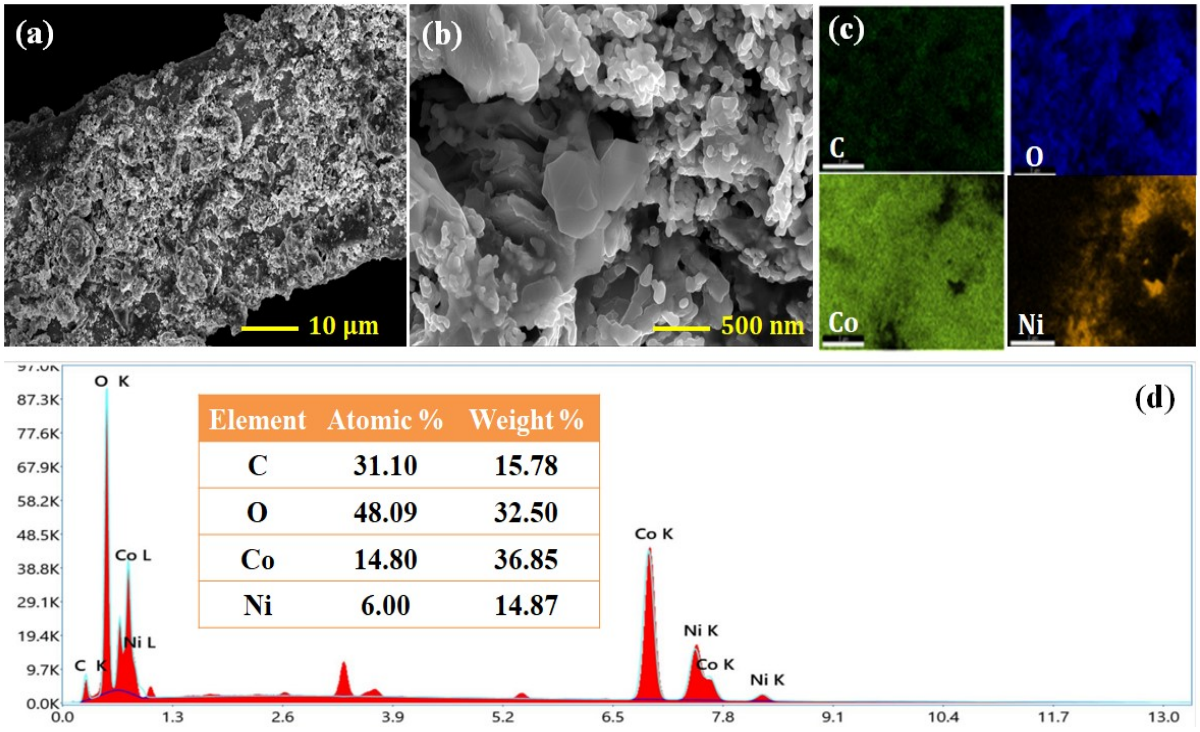

Element	Atomic %	Weight %
C	31.10	15.78
O	48.09	32.50
Co	14.80	36.85
Ni	6.00	14.87

Figure S12: XRD of Co-O-C/CPs after OER and HER

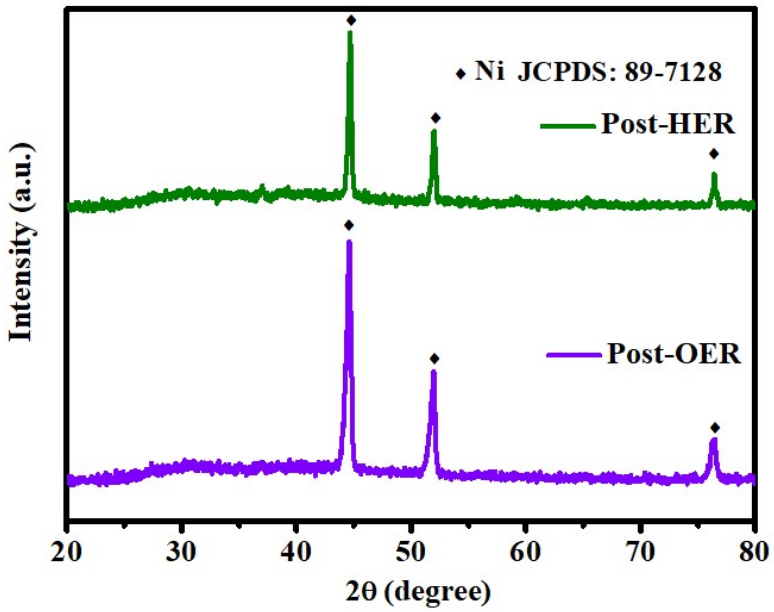

Figure S13: Post XPS of Co-O-C/CPs: (a) Co 2p after OER and (b) Co 2p after HER

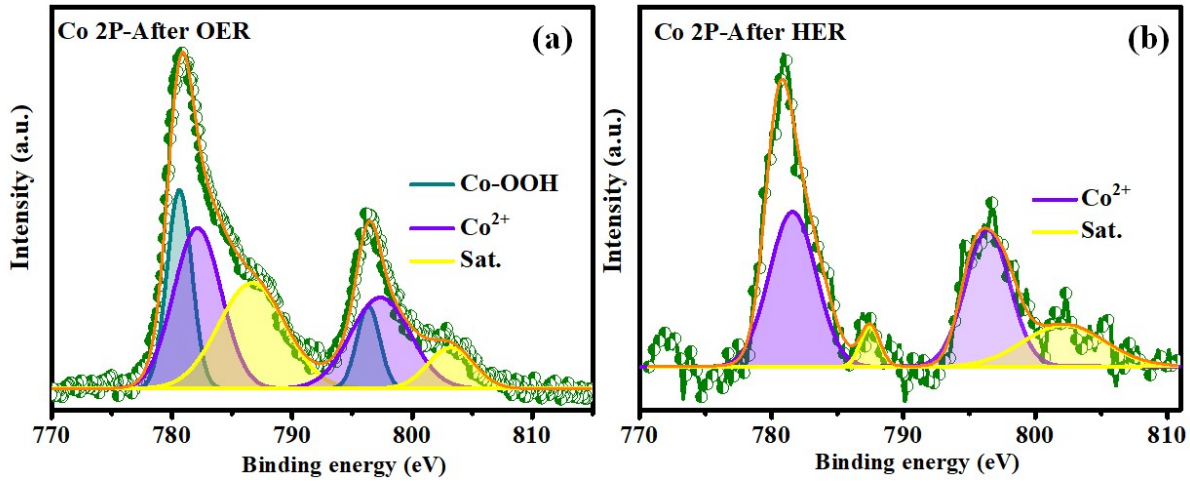

Figure S14: Post XPS of Co-O-C/CPs: (a) C 1s after OER and (b) C 1s after HER

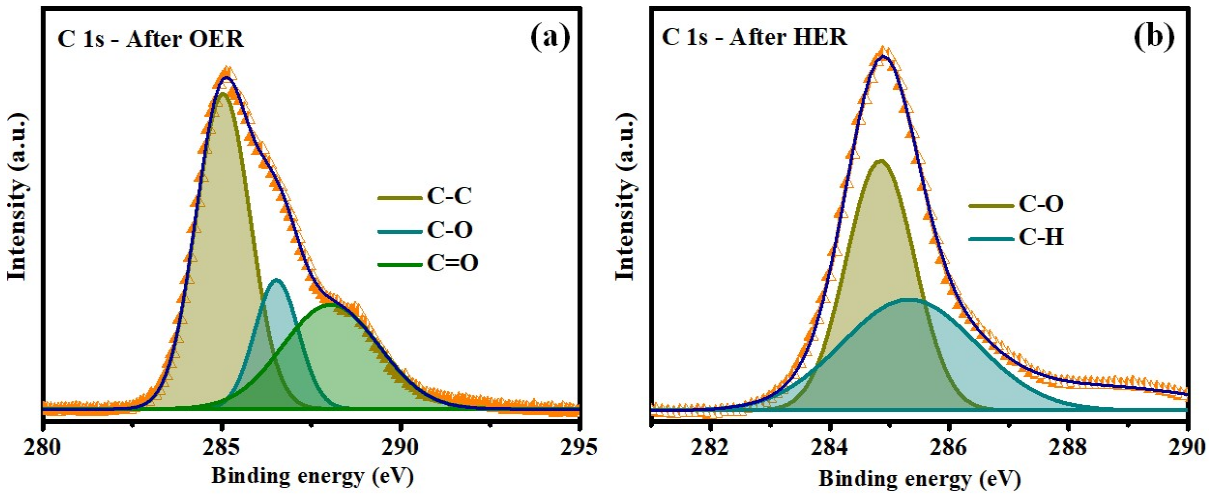

Figure S15: Post XPS of Co-O-C/CPs: (a)O 1s after OER and (b)O 1s after HER

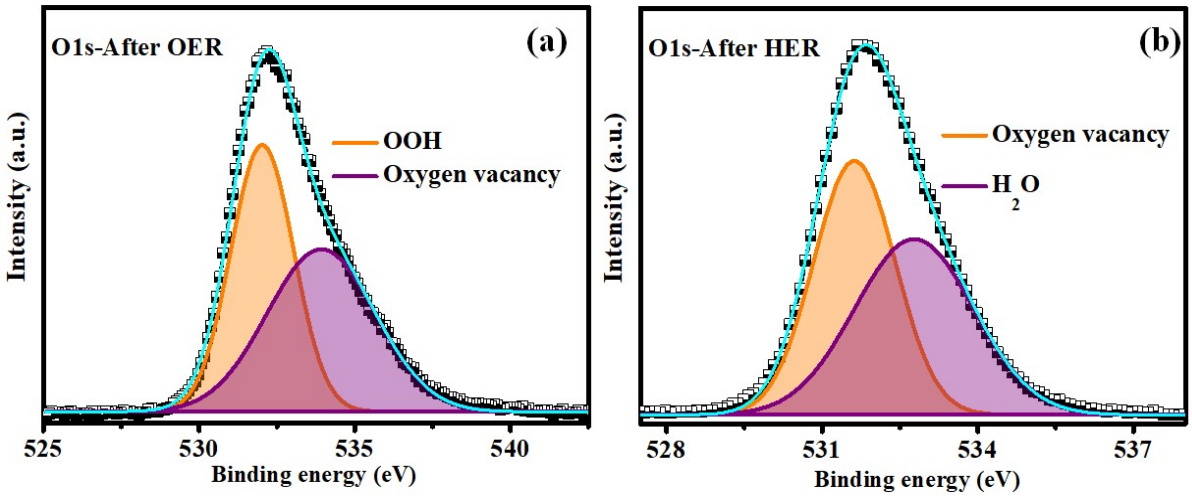

SI-III: Calculations

SI. C1. Energy calculation

Amount of energy released = combustion of glucose * no. of moles of glucose burned

= 2808 kJ * 0.00556

= 156.12 kJ.

SI:C2. Scherrer equation

$D_{hkl} = 0.9\ \lambda / (\beta_{hkl} \cos\theta)$

where D_{hkl} - crystallite size, λ - X-ray wavelength (Cu, Kα1), θ - diffraction angle, and β_{hkl} - full width at half maximum of the diffraction peak.

SI. C3. Tafel equation

$\eta = a + b \log J$,

where η is the overpotential (V vs. RHE), b the Tafel slope, and j the corresponding current density (mA /cm^2) as well as the Tafel constant

SI. C4. ECSA calculation

The capacitive currents are measured in a potential range where no faradic processes occur. The sweep potential is between 0.40 to 0.50 V vs. RHE at different scan rates (40, 60, 80, 100, 120 and 140 mV s^{-1}). The differences in current density variation ($\Delta j = j_a - j_c$) at the potential of 0.45 V vs. RHE plotted against scan rate are fitted to estimate the electrochemical double layer capacitances (C_{dl}), which are used to estimate the electrochemical surface area (ECSA).

$$ECSA = C_{dl} / C_s$$

Where double layer capacitance is C_{dl} and specific capacitance is C_s, and 40 μF cm^{-2} is a constant to convert capacitance to ECSA. The specific capacitance can be converted into an electrochemical active surface area (ECSA) using the specific capacitance value for a flat standard with 1 cm^2 of real surface area.

SI. C5. Turnover frequency (TOF) calculation

The TOF is defined as the number of H_2 or O_2 molecules evolved per site per second

$$\text{TOF of } O_2 \text{ or } H_2 = \frac{J * A}{z * f * n}$$

where, J- Current density (mA/cm^2), A- Geometric surface area of the working electrode, z - no. of electrons involved in the OER and HER process, F- Faraday Constant (96485.3 C mol^{-1}) and n- The number of moles of active sites on the electrode.

SI. C6. Faradaic efficiency

Faradaic efficiency of Co-O-C/CPs was calculated by dividing the amount of the experimentally generated gas by the theoretical amount of gas which is calculated by the charge passed through the electrode:

$$\text{Faradic efficiency (\%)} = \frac{\text{(Number of moles of gas produced experimentally for a certain time)} * 100}{\text{Theoretically calculated gas production (in mole) for the same time}}$$

The theoretical amount of gas (O_2 and H_2) was calculated from accumulated charge during galvanostatic electrolysis by assuming 100% faradic efficiency. Theoretical amount (n in mole) of gas (H_2, O_2) = Q / (n * F) = (I * t) / (n * F) where Q is the summation of the charge passed through the electrodes, n is the number of electrons which is 2 for HER and 4 for OER and F is the Faraday constant (96485.3 C.mol^{-1}).

SI. C7. Calculation of hydrogen generation

Based on the displaced amount of water due to the hydrogen bubbles, the amount of hydrogen generated was calculated using the below relationships.

Amount of hydrogen generated in 1 h = amount of water displaced in litres (1)

$$\text{Amount of hydrogen generated in moles for 1 h} = \frac{\text{Amount of water displaced (litres)}}{\text{22.4 litres}} \quad (2)$$

We also calculated the hydrogen generation rate from the electrical charge passed through the electrode using the equation given below.

$$\left(\begin{array}{c}\text{Current obtained during}\\ \text{water electrolysis}\end{array}\right) \text{X} \left(\begin{array}{c}\text{Time duration for}\\ \text{each potential}\end{array}\right) = \text{Coulomb} \quad (3)$$

$$\frac{\text{Coulomb x F}}{\text{96485 C}} = \text{No. of moles of } e^- \text{ for } H_2 \text{ generation} \quad (4)$$

$$\frac{\text{No. of moles of electron for } H_2 \text{ generation x 1 mole of } H_2 \text{ gas}}{\text{2 moles of electron}} = \begin{array}{c}\text{Moles of Hydrogen}\\ \text{generated}\end{array} \quad (5)$$

SI-IV Tables and reference

SI: T1- Comparison of HER performance of Co-O-C/CPs with other reported metal carbide electrocatalysts.

S.No	Catalyst	Electrode	η_{10}-HER (mV)	Reference
1	**Co-O-C/CPs**	**NF**	**115**	**This work**
2	Co_3C-NB	GCE	154	*J. Mater. Chem. A,* 2019, **7**,14904-14915
3	MoC-Mo_2C	GCE	120	*Nano Energy,* 2021, **90**, 106533
4	p-WCx NWs	CC	122	*J. Mater. Chem. A,* 2017, **5**, 13196 -13203
5	vMoxC	GCE	116	*ACS nano,* 2020, **14**, 4988 - 4999.
6	α-Mo2C	GCE	160	*J. Mater. Chem. A*, 2015, **3**, 8361 - 8368.
7	Ni-GF/VC	NF	128	*Adv. Energy Mater.,* 2020, **10**, 2002260
8	Mo_2C/NC	GCE	148	*Int. J. Hydrogen Energy,* 2018, **43**, 17244 -17251.
9	WC@NG/CNT,	-	253	*Adv. Funct. Mater.,* 2022, **32**, 2108167
10	$(Ni_{0.2}Co_{0.8})_6Mo_6C_2$	GCE	100	*Mater. Adv.,* 2021, **2**, 336 - 344.
11	W_2C-HS	GCE	153	*ACS omega,* 2019, **4**, 4185 - 4191.

SI: T2- Comparison of OER performance of Co-O-C/CPs with other reported metal carbide electrocatalysts.

S.No	Catalyst	Electrode	η_{10}-OER (mV)	Reference
1	**Co-O-C/CPs**	**NF**	**240**	**This work**
2	Co/Mo_2C	CC	366	*Int. J. Hydrogen Energy,* 2020, **45**, 21221 - 21231.
3	FeNi–Mo_2C/C	GCE	288	*Nano Energy,* 2021, **88**, 106216
4	$Co_6Mo_6C_2$/NCRGO	GCE	260	*ACS Appl. Mater. Interfaces,* 2017, **9**, 16977 -16985.
5	CoOx@CN	GCE	260	*J. Am. Chem. Soc.*, 2015, **137**, 2688-2694.
6	CoP/rGO-400	RDE	340	*Chem. Sci.,* 2016, **7**, 1690 -1695.
7	Ni/Mo_2C-PC	GCE	368	*Chem. Sci.,* 2017, **8**, 968-973.
8	Ni_3C/C	CFP	320	*Adv. Mater.,* 2016, **28**, 3326 -3332.
9	$Fe_3C@NG_{800\text{-}0.2}$	RDE	361	*ACS Appl. Mater. Interfaces,* 2015, **7**, 21511-21520.
10	$NiCo_2S_4$	NF	260	*Adv. Funct. Mater.,* 2016, **26**, 4661-4672.
11	Co_3ZnC/Co@CN	GCE	366	*J. Mater. Chem. A,* 2016, **4**, 9204-9212.

SI: T3- Comparison of overall water splitting performance of Co-O-C/CPs with other reported metal carbide electrocatalysts.

S.No	Catalyst	Electrode	Cell Potential (V)	Reference
1	**Co-O-C/CPs**	**NF**	**1.60**	**This work**
2	Mo_2C@CS	GCE	1.73	*ChemSusChem,* 2017, **10**, 3540 -3546
3	β-Mo_2C	NF	1.65	*Electrochim. Acta,* 2019**, 298**, 305 -312.
4	Co_6W_6C@NC	CC	1.58	*Small,* 2020, **16**, 1907556
5	Ni/Mo_2C-PC/NF	NF	1.66	*Chem. Sci.,* 2017, **8**, 968 -973.
6	Ni−Mo_xC/NC-100	GCE	1.72	*ACS Appl. Mater. Interfaces,* 2018, **10**, 35025 -35038.
7	$NiCo_2N$	NF	1.70	*ChemSusChem,* 2017, **10**, 4170 -4177.
8	$Co_6Mo_6C_2$	GCE	1.81	*Chem. Eur. J.,* 2020, **26**, 4157 -4164.
9	Co/W-C@NCNSs	GCE	1.68	*Nano Energy,* 2019, **57**, 746-752.
10	Co-NC@Mo_2C	GCE	1.685	*Green Energy and Technology,* 2019, 539
11	$Ni_3ZnC_{0.7}$/NCNT	NF	1.66	*Carbon,* 2019, **148**, 496 -503.